Development Advance Online Articles. First posted online on 17 March 2016 as 10.1242/dev.130211
Access the most recent version at http://dev.biologists.org/lookup/doi/10.1242/dev.130211

DRACULA2, a dynamic nucleoporin with a role in the regulation of the shade avoidance syndrome in Arabidopsis.

Marçal Gallemí[1*,£], Anahit Galstyan[1*,¥], Sandi Paulišić[1], Christiane Then[1,§], Almudena Ferrández-Ayela[2], Laura Lorenzo-Orts[1], Irma Roig-Villanova[1], Xuewen Wang[3,¶], Jose Luis Micol[2], Maria Rosa Ponce[2], Paul F. Devlin[3], Jaime F. Martínez-García[1,4©]

[1]Centre for Research in Agricultural Genomics (CRAG), CSIC-IRTA-UAB-UB, Campus UAB, Barcelona, Spain; [2]Instituto de Bioingeniería, Universidad Miguel Hernández, Campus de Elche, Elche, Spain; [3]School of Biological Sciences, Royal Holloway University of London, Egham, Surrey, United Kingdom; [4]Institució Catalana de Recerca i Estudis Avançats (ICREA), Ps. Lluís Companys 10, Barcelona, Spain.

*These authors contributed equally to this work and order was selected randomly.

[£]Current address, Institute of Science and Technology Austria, Klosterneuburg, Austria; [¥]Current address, Department of Comparative Development and Genetics, Max Planck Institute for Plant Breeding Research, Cologne, Germany; [§]Current address, INRA, Joint Research Unit "Biology and Genetics of Plant-Pathogen Interactions", Campus International de Baillarguet, Montpellier, France; [¶]Current address, Institute of Botany, Chinese Academy of Sciences, Kunming, China.

© Corresponding author, E-mail, jaume.martinez@cragenomica.es

ABSTRACT

When plants grow in close proximity, basic resources such as light might become limiting. Under such conditions, plants respond to anticipate and/or adapt to the light shortage, a process known as the shade avoidance syndrome (SAS). After a genetic screening using a shade-responsive luciferase reporter line (PHYB:LUC), we identified *DRACULA2* (*DRA2*) that encodes an Arabidopsis homolog to mammalian nucleoporin 98, a component of the nuclear pore complex (NPC). DRA2, together with other nucleoporines, positively participates in the control of the hypocotyl elongation response to plant proximity, a role that can be considered as dependent on the nucleocytoplasmic transport of macromolecules (i.e., transport-dependent). In addition, our results reveal a specific role for DRA2 in controlling shade-induced gene expression. We suggest that this novel regulatory role of DRA2 is transport-independent, and it might rely on its dynamic localization in and off the NPC. These results provide mechanistic insights on how SAS responses are rapidly established by light conditions. They also indicate that nucleoporins have an active role in plant signaling.

INTRODUCTION

As sessile organisms, plants cannot move to the best places to grow: therefore, they either adapt or die. One unfavorable situation is to grow in crowded conditions (e.g., those found in forests, prairies or agricultural communities), since the close proximity of neighboring plants can result in competition for limited resources, such as light. The shade avoidance syndrome (SAS) comprises the set of plant responses aimed to adapt growth and development to high plant density environments. Neighboring plants selectively absorb red light (R) and reflect far-red light (FR), resulting in a moderate reduction in the R to FR ratio (R:FR). Under plant canopy shade, the concomitant reduction in light intensities results in even lower R:FR ratios. In either case, these changes become a signal perceived by the R- and FR-absorbing phytochrome photoreceptors (Smith, 1982; Smith and Whitelam, 1997; Keuskamp et al., 2010; Martinez-Garcia et al., 2010). In *Arabidopsis thaliana* (from now on Arabidopsis), a gene family of five members (*PHYA-PHYE*) encodes the phytochromes (Bae and Choi, 2008), which have positive (phyB-phyE) and negative (phyA) roles in controlling SAS-driven development (Franklin, 2008; Martinez-Garcia et al., 2010; Martinez-Garcia et al., 2014). Phytochromes exist in two photoconvertible forms, an inactive R-absorbing Pr form and an active FR-absorbing Pfr form. Under sunlight (i.e., a high R:FR ratio), the photo-equilibrium is displaced towards the active Pfr forms, and SAS is suppressed. Under a low R:FR ratio, phytochrome photo-equilibrium is displaced towards the inactive Pr forms, and SAS is induced by affecting the interaction with PHYTOCHROME INTERACTING FACTORs (PIFs) and altering their stability and/or activity (Smith and Whitelam, 1997; Martinez-Garcia et al., 2000; Lorrain et al., 2008; Leivar and Quail, 2011), which results in rapid changes in the expression of

dozens of *PHYTOCHROME RAPIDLY REGULATED* (*PAR*) genes (Salter et al., 2003; Roig-Villanova et al., 2006; Roig-Villanova et al., 2007; Lorrain et al., 2008). Because most of these *PAR* genes encode transcriptional regulators, it is assumed that SAS responses are a consequence of the regulation of a complex transcriptional network by phytochromes (Bou-Torrent et al., 2008; Josse et al., 2008). Indeed, genetic approaches have demonstrated regulatory roles in SAS for a large number of *PAR* genes encoding transcriptional regulators, including members of at least 3 different families: basic-helix-loop-helix (HFR1, PAR1, PAR2, BIMs and BEEs), homedomain-leucine zipper (HD-ZIP) class II (ATHB2, ATHB4, HAT1, HAT2 and HAT3), and B-BOX-CONTAINING (BBX). PIF stability and/or activity was also shown to be increased by low R:FR perception (Lorrain et al., 2008; Li et al., 2012). Genetic analyses unraveled roles for these factors on the negative (including BBX21, BBX22, HFR1, PAR1, PAR2 and PIL1) or positive regulation of SAS (including BBX24, BBX25, PIFs, BIMs and BEEs) (Sessa et al., 2005; Roig-Villanova et al., 2006; Roig-Villanova et al., 2007; Crocco et al., 2010; Cifuentes-Esquivel et al., 2013; Gangappa et al., 2013; Bou-Torrent et al., 2015). Therefore, the low R:FR perception rapidly changes the balance of positive and negative factors, resulting in the appropriate SAS responses.

Phytochromes are known to partition between the cytoplasm and nucleus (and even within the nucleus) in a light dependent manner; similarly, after low R:FR exposure, newly formed and shade-stabilized PIFs rapidly reach the nucleus. To do so these proteins have to cross the nuclear envelope, a physical barrier that separates both cell compartments. The nuclear pore complex (NPC) is a large multiprotein complex that is the sole gateway of macromolecular trafficking between the cytoplasm and the nucleus. Despite structural differences, there are conserved functional similarities between NPCs from plants and other organisms (Raices and D'Angelo, 2012; Parry,

2013; Tamura and Hara-Nishimura, 2013). The NPC consists of multiple copies of at least 30 different nucleoporines (NUPs), which together form a channel-like structure of octagonal-symmetry organized in three elements: a nuclear basket, a central pore, and cytoplasmic fibrils. Depending on their position within the NPC, NUPs can be classified into two major categories: scaffold (which form the rigid skeleton) and peripheral (which form a selective barrier for the diffusion of molecules larger than ~60 KDa). Proteomic approaches have identified several Arabidopsis NUPs belonging to both categories (Tamura et al., 2011). Functionally, Arabidopsis NUP-deficient single mutant lines display several pleitropic developmental alterations, such as early flowering, disrupted circadian function and even embryo lethality (MacGregor et al., 2013; Parry, 2014). However, whether the NPC and/or individual NUPs impact photomorphogenic responses and/or light signaling remains virtually unexplored.

To identify new regulatory components of the SAS, a high-throughput genetic screen was performed after EMS mutagenesis of a shade-responsive luciferase reporter line, PHYB:LUC (hereafter PBL), which expresses the *LUCIFERASE* (*LUC*) gene under the control of the Arabidopsis *PHYB* promoter in the Ws-2 genetics background (Kozma-Bognar et al., 1999). As a result we identified *dracula* (*dra*) mutants, causing an attenuated luciferase response to low R:FR light. One of the mutants identified was *dracula1* (*dra1*), which carries the novel $phyA^{G773E}$ mutation (Wang et al., 2011). Here, we present *dra2*, which affects a gene encoding NUP98a, a component of the NPC in plants (Xu and Meier, 2008; Tamura et al., 2011). Our results suggest that an intact NPC is essential for proper SAS responses. Furthermore, our comparative analyses of several NUP-deficient mutant seedlings indicate that DRA2 has also a specific role in the early shade-regulation of *PAR* expression.

RESULTS AND DISCUSSION

The *dra2-1* mutation alters SAS seedling response

After EMS mutagenesis of the PBL reporter line, we performed a large-scale screen looking for mutant seedlings exhibiting significant altered luciferase activity after 2 h of simulated shade ($P<0.001$) (Wang et al., 2011). One of the mutants isolated, *dra2-1*, showed an attenuated luciferase activity after just 1 h of W+FR treatment (Figure 1A). Additional molecular analyses (see below) indicated that *LUC* expression in response to shade was attenuated in *dra2-1*. Adult *dra2-1* plants grown under standard greenhouse (long day) conditions displayed a range of morphological phenotypes, such as small rosettes, short flowering stems and siliques and a general weak aspect; moreover, these plants were early flowering under both long- and short-day conditions (Figure S1A-C). Mutant seedlings grown under continuous white light (W) had long hypocotyls and strongly hyponastic cotyledons (Figure 1B). More importantly, the seedling response to W+FR in terms of hypocotyl, cotyledon and primary leaf elongation was attenuated in *dra2-1* compared to PBL (Figures 1C, S1D).

DRA2 encodes Arabidopsis NUP98a

Genetic analyses indicated that the mode of inheritance of the *dra2-1* line is monogenic and recessive. After positional cloning, a candidate interval of 270 kb at the upper arm of chromosome 1, flanked by the nga63 (between the At1g09910 - At1g09920 genes) and cer458005 (At1g10560 - At1g10570) markers, was defined (Figure S2A). While this work was in progress we learned that mutant alleles of Arabidopsis genes encoding NUPs displayed long hypocotyls and/or early-flowering phenotypes (Ferrandez-Ayela et al., 2013; Parry, 2013; Tamura and Hara-Nishimura, 2013). At1g10390, a gene within the candidate interval annotated to encode a NUP, was

sequenced in *dra2-1* and PBL. In *dra2-1* plants, At1g10390 carries a G to A transition, which would result in a nonsense mutation at Trp^{780} of the protein (Figure S1E). From now on, and based in results shown below, we will refer to this gene as *DRA2*. First, cosegregation analyses of the mutant phenotype and the identified mutation indicated that the only allele detected among the phenotypically mutant seedlings was *dra2-1*, a result consistent with the recessive nature of this mutant (Figure S1F). Second, the recessive *dra2-1* mutation was complemented with a constitutively expressed translational fusion of *DRA2* to the *GREEN FLUORESCENT PROTEIN* (*GFP*) marker gene (35S:DRA2-GFP lines) at both the seedling and the adult stages (Figures 1D, S2B-D). And third, transgenic seedlings overexpressing an RNAi directed towards *DRA2* (35S:RNAi-DRA2 lines, generated in the Ws-2 background) showed a similar phenotype of *dra2-1* seedlings. This RNAi was directed towards a region that diverged between *DRA2* and its closest homologue in the Arabidopsis genome (At1g59660) that we named as *DRA2-LIKE* (*DRAL*) (Figure S3A). The strong hyponastic cotyledons characteristic of *dra2-1* seedlings was only observed in a few 35S:RNAi-DRA2 lines that either had severe growth problems and died before producing seeds or lost their characteristic phenotype in the following generation (Figure S3B). Nonetheless, transgenic seedlings with a mild phenotype had longer hypocotyls than Ws-2 under W; importantly, in these lines the hypocotyl response to W+FR was attenuated compared to Ws-2 (Figures 1E, S3C). Together, these results indicated that At1g10390 is the causal gene for the phenotype of *dra2-1*.

Lines carrying T-DNA insertions disrupting At1g10390 were identified in the Col-0 background. We named these mutants as *dra2-2* to *dra2-5*. In these lines, except *dra2-2*, T-DNA insertions mapped within the main ORF, and are likely to perturb DRA2 function (Figure S4A). At least one of these alleles is null, as indicated by the

absence of detectable *DRA2* mRNA in *dra2-4* seedlings (Figure S4B). Nonetheless, all analyzed *dra2* mutant seedlings had longer hypocotyls than Col-0 under W. However, they did show an almost wild-type response to simulated shade, in contrast with *dra2-1* seedlings (Figures 1F, S4C). Overall, these T-DNA mutants identified in Col-0 displayed a mild or weak phenotype, a result consistent with published information about an additional knock-out allele of *DRA2* (Parry, 2014). The strong phenotype shown by the *dra2-1* mutant, particularly its hyponastic cotyledons, was severely reduced after four *dra2-1*xCol-0 backcrosses (Figure S4D). These results suggested that the genomic Col-0 background (very likely near the *DRA2* locus) strongly modifies the mutant phenotype caused by *DRA2* loss of function.

DRA2 encodes a NUP containing phenylalanine-glycine (FG) repeats of 1041 amino acids and a molecular mass of about 105 kDa (Xu and Meier, 2008; Tamura and Hara-Nishimura, 2013). A number of yeast and vertebrate NUPs have FG repeats, which are thought to provide transient, low-affinity binding sites for transport receptors. Two genes encoding a NUP-like FG-repeat-containing protein can be identified by sequence similarity searches with mammalian Nup98 (mNup98) in the Arabidopsis database: *DRA2* (*At1g10390*, *NUP98a*) and *DRAL* (*At1g59660*, *NUP98b*) (Xu and Meier, 2008). Proteomic analyses of the NPC identified several Arabidopsis NUPs, including DRA2 and DRAL (Tamura et al., 2011). The N-terminal region of mNup98 (NtNup98) contains 39 FG repeats (Table S1) (Radu et al., 1995; Griffis et al., 2002). The C-terminal region of mNup98 (CtNup98) mediates its interaction with the NPC (Hodel et al., 2002) and contains a minimal cleavage domain that is evolutionarily conserved also in the C-terminal part of Arabidopsis DRA2 and DRAL proteins, which suggests that the C-terminal region of DRA2 mediates the interaction with the NPC in plants. Overexpression of mammalian NtNup98 fused to GFP resulted in a dominant

negative form that interfered with the endogenous mNup98 activity (Liang et al., 2013). Overexpression of the N-terminal part of *DRA2* (encoding for amino acids 1 to 779) fused to the *GFP* in Col-0 (35S:NtDRA2-GFP lines) caused stunted growth. More importantly, transgenic seedlings had slightly longer hypocotyls than Col-0 under W and displayed an attenuated response to simulated shade (Figure 1G), a phenotype resembling that of the strong *dra2-1* and 35S:RNAi-DRA2 seedlings. The NtDRA2 fragment contains all FG repeats and seems unable to bind to the NPC (Table S1), suggesting that NtDRA2 might also behave as a dominant negative form towards DRA2 in the Col-0 background. Interference of NtDRA2 with the function of DRAL might further explain the more severe phenotype of these transgenic lines compared to the single null *dra2* mutants in the Col-0 background.

Loss of function of different NUPs causes an altered hypocotyl response to simulated shade

To evaluate whether the sole disruption of NPC function results in an altered SAS phenotype, we tested mutants affected in several other NUPs, such as SUPPRESSOR OF AUXIN RESISTANCE1 (SAR1)/NUP160 (hereafter SAR1), SAR3/NUP96 (hereafter SAR3) (Parry et al., 2006), TRANSCURVATA1 (TCU1)/NUP58 (hereafter TCU1) (Ferrandez-Ayela et al., 2013), NUP54 and NUP62 (Figure S5). Structurally, these Arabidopsis NUPs contain different domains: SAR1 and SAR3 contain an α-solenoid domain; SAR1 also contains a β-propeller; NUP54, TCU1, NUP62 and DRA2 contain FG repeats; and NUP54, TCU1 and NUP62 also contain a coiled-coil region (Tamura and Hara-Nishimura, 2013). Functionally, these NUPs represent different types of components of the NPC: SAR1 and SAR3 are predicted to be scaffold NUPs; and NUP54, TCU1 and NUP62, together with DRA2, are considered

to be peripheral NUPs attached to the membrane-embedded scaffold (D'Angelo et al., 2009; Tamura and Hara-Nishimura, 2013). After analyzing the hypocotyl response to W and W+FR, mutant alleles were classified as displaying mild (*sar3-3*, *nup54-1*, *nup54-2*, *tcu1-2* and *tcu1-4*) or strong (*sar1-4*, *sar3-1*, *nup62-1*, *nup62-2* and *tcu1-1*) phenotypes compared to the response of the corresponding wild-type seedlings (Figures 2A-D, S5). The mild alleles mimicked the response of *dra2-2* to *dra2-5* mutants (in the Col-0 background), whereas the strong alleles responded similar to *dra2-1* (an allele in the Ws-2 background). Similar to that, the phenotypic strength of loss-of-function *tcu1* alleles was affected by the genetic background: *tcu1-2* and *tcu1-4* (in Col-0) were mild whereas *tcu1-1* (in L*er*) was strong (Figures 1, S4). We hypothesized that the genetic background influence could be due to different levels of impairment of NPC activity, likely caused by variations in the basal NUP activity in the compared accessions. Indeed, an increase in the phenotype severity has been observed by other authors in double NUP mutants (Ferrandez-Ayela et al., 2013; Parry, 2014), suggesting a relationship between the strength of the phenotypes analyzed and the level of impairment of the NPC function. Consistently, double mutants involving weak alleles of *DRA2* (e.g., *dra2-3*, *dra2-4* and *dra2-5*) and *TCU1* (*tcu1-2*) showed a shade-induced hypocotyl response similar to that of single mutants carrying strong alleles (Figures 2E, S5F).

DRA2 participates in the mRNA export from the nucleus

SAR1 and SAR3 were reported to participate in mRNA export from the nucleoplasm to the cytoplasm (Dong et al., 2006; Parry et al., 2006). To address whether DRA2 also participates in this transport-related activity of the NPC, *in situ* hybridization to localize poly(A)-mRNA was carried out in 7-day-old wild-type and

NUP mutant seedlings. Using an oligo(dT)50 probe, end-labeled with fluorescein, nuclear retention of poly(A)+ RNA was clearly discernible in seedlings of the strong alleles *sar3-1* and *dra2-1*, but not in the corresponding wild-type and the weak *dra2-3* and *dra2-4* mutants (Figure 3A). These results suggested that DRA2 is required for mRNA nucleocytoplasmic trafficking in a genetic background-dependent manner and support that *dra2-1* seedlings have an impaired NPC.

Expression of *DRAL*, the closest paralog of *DRA2*, was found to be strongly upregulated (18 fold) in *dra2-1* seedlings (Figure 3B), but only moderately increased (3 fold) in weak *dra2-4* mutant seedlings (Figure S6). *DRAL* expression was also upregulated in single or double NUP-deficient mutants with strong phenotypes, such as *sar1-4* (10 fold), *sar3-1* (14 fold), *tcu1-1* (7 fold) and *dra2-4;tcu1-2* (11 fold), and to a lesser extent in the weak *tcu1-2* (2-3 fold) and *sar3-3* (3 fold) mutants (Figures 3B, S6). *DRAL* expression was also strongly upregulated in RNAi-DRA2 seedlings with downregulated *DRA2* expression (Figure 3C). A significant increase in the expression of *DRAL* and other genes involved in nuclear transport, such as *RNA EXPORT FACTOR 1* (*RAE1*) and *NUCLEAR EXPORTIN 1B* (*XPO1B*), was recently reported in seedlings of three different NUP-deficient mutants: *nup62-2*, *nup160-1* (a mutant allele of *SAR1* not analyzed in our work) (Parry, 2014) and *high expression of osmotically responsive genes 1* (*hos1*) (MacGregor et al., 2013). These results revealed a possible feedback relationship between an impaired NPC function and the expression of genes involved in nuclear transport (Parry, 2014). Although it is unclear if this feedback regulation has any biological relevance, e.g., if it results in a compensatory mechanism to increase the rate of nuclear transport, our observations do indicate a positive correlation between *DRAL* expression levels and the strength of the physiological SAS phenotype. Since the strong mutants analyzed display a clear poly(A)+ RNA nuclear

retention that reflects defects in the NPC (Figure 3A) (Dong et al., 2006; Parry et al., 2006), our results support that *DRAL* upregulation is a reliable marker for NPC dysfunction.

Mutant *dra2-1* seedlings display an attenuated early induction of *PAR* gene expression

We reasoned that other shade-regulated responses, such as induction of *PAR* gene expression, may also be altered in NUP-deficient mutants. We therefore analyzed the accumulation of transcripts of shade-responsive genes in *dra2-1* and PBL seedlings before and after W+FR exposure (0, 1, 2 and 4 h). As expected, the transgenic marker *LUC* and the endogenous *PHYB*, *PIL1* and *HFR1* were rapidly induced after W+FR treatment. However, their shade-induced expression was significantly attenuated in *dra2-1* compared to PBL control seedlings (Figure 4A) indicating that DRA2 promotes the shade-induced expression of these genes. *ATHB2*, another well-known shade-induced gene, was unaffected by simulated shade in *dra2-1* seedlings (Figure S7). In *sar1-4* and *sar3-1* seedlings, *PHYB* shade-induced expression was also attenuated compared to the Col-0 control, whereas that of *PIL1* and *HFR1* was enhanced (rather than reduced) (Figure 4B; Table S2). Therefore we deduced that SAR1 and SAR3 participate like DRA2 in promoting the shade-triggered activation of *PHYB* expression, but differ from DRA2 in their specific effect of *PIL1* and *HFR1* gene expression. No significant differences in the early shade-induced expression of these genes were found between wild-type (L*er*) and strong *tcu1-1* mutant seedlings (Figure 4C). These observations indicate that (i) rapid and efficient shade-induced gene expression requires specific NUPs, such as DRA2, SAR1 and SAR3, and (ii) these NUPs appear to have different roles in this process.

Several of the Arabidopsis NUP-deficient single mutant lines are early flowering, including the strong *sar1*, *sar3* (Dong et al., 2006; Parry et al., 2006), *tcu1* (Ferrandez-Ayela et al., 2013), *nuclear pore anchor* (nua, also known as *tpr*) (Jacob et al., 2007; Xu et al., 2007), *nup136* (Tamura et al., 2011), *nup62* (Zhao and Meier, 2011), *hos1* (MacGregor et al., 2013) and *dra2* mutants (Figure S1). More recently, analyses of NUP-deficient mutants, such as *hos1*, *sar1*, *nua* and *nup107* also showed disrupted circadian function and cold-regulated gene expression, suggesting that these additional phenotypes are also a general consequence of disrupting NPC function in plants (MacGregor et al., 2013). Our analyses indicated that some of these mutants share additional phenotypes, such as upregulation of *DRAL* expression, long hypocotyls under W and/or attenuated hypocotyl elongation in response to simulated shade (Figures 1-3, S5, S6). The shared pleiotropic phenotypes of different NUP-deficient mutants is a likely consequence downstream of a generic disruption of the NPC and the associated effect on its main function, the nucleocytoplasmic trafficking. These phenotypes can therefore be referred to as transport-dependent (Capelson and Hetzer, 2009; Raices and D'Angelo, 2012).

By contrast, the attenuation of the early shade-triggered gene expression is not a general phenomenon caused by an unspecific depletion of any NPC component. Indeed, whereas loss of TCU1 had no impact at all on *PAR* expression in response to low R:FR, other NUPs (SAR1, SAR3 and DRA2) modulated shade-induced expression of specific genes in similar or even opposite directions, as it was observed in *dra2-1*, *sar1-4* and *sar3-1* seedlings (Figure 4). These results support that a number of different plant NUPs have specific roles in the control of gene expression besides their transport-dependent fnctions as components of the NPC. Indeed, an increasing body of evidence (largely from studies in yeast and mammals) suggests that some NUPs are also involved in

regulating gene expression, a role that has been referred to as transport-independent (Capelson and Hetzer, 2009; Raices and D'Angelo, 2012). In particular, animal Nup98 appears to regulate gene expression by binding directly the chromatin and/or by stabilizing some mRNAs in cell cultures (Capelson et al., 2010; Kalverda et al., 2010; Singer et al., 2012). This is proposed to occur because mNUP98 is dynamic, i.e., it is associated with the NPC and shuttles between the nucleus and the cytoplasm (Griffis et al., 2002). In plants, only Nup136 was shown to be dynamic, although this feature was not related with any transport-independent activity such as regulation of specific genes (Tamura et al., 2011).

DRA2 is a dynamic NUP

A translational fusion between GFP and mNup98 was reported to move between the nucleoplasm and the NPC, as well as between the nucleus and the cytoplasm, concluding that this is a dynamic NUP (Powers et al., 1997; Fontoura et al., 2000; Griffis et al., 2002). This dynamism appears to be related with the role of mNUP98 in gene regulation (i.e., it is transport-independent), since the mobility of mNup98 within the nucleus and at the NPC is dependent on ongoing transcription by RNA polymerases (Griffis et al., 2002; Raices and D'Angelo, 2012). mNup98 localized in the nucleoplasm and the cytoplasm can associate with some spots (mostly nuclear) of unknown identity. The GFP-fusion of the animal N-terminal Nup98 (NtNup98-GFP) is also localized preferentially in spots within the nucleus (Griffis et al., 2002; Kalverda et al., 2010). Similarly, transient overexpression of *NtDRA2-GFP* in leek epidermal cells resulted in GFP activity in both cytoplasmic and nuclear spots (Figure 5A). Arabidopsis 35S:NtDRA2-GFP seedlings also displayed fluorescence in cytoplasmic- and nuclear-localized spots (Figure 5B).

In 35S:NtDRA2-GFP seedlings, *DRAL* expression was also significantly upregulated (8 fold), indicating that overexpression of *NtDRA2* interferes with the transport-dependent activity of the NPC. More importantly, shade-induced *HFR1* and *PIL1* expression was also significantly attenuated (Figure 5C), suggesting that this truncated form also interferes with transport-independent activities of DRA2. These results support our hypothesis that the FG-containing NtDRA2 fragment has a dominant negative effect on the expression of DRA2-regulated genes, an activity also observed for the N-terminal mNup98 fragment (Liang et al., 2013). Since NtDRA2 does not localize in the NPC, it should interfere with pools of DRA2 that localize either in the nuclei or the cytoplasm.

To verify DRA2 subcellular localization, we aimed to use our 35S:DRA2-GFP lines. While high levels of *DRA2* expression were detected in these lines (Figure S8A) and the DRA2-GFP fusion was active to complement *dra2-1* mutation (Figure 1D), no GFP fluorescence was detected in these seedlings. Leaves of *Nicotiana benthamiana* agroinfiltrated to transiently overexpress *DRA2-GFP* also lacked any detectable GFP fluorescence (Figure 6A). The C-terminal end of DRA2 contains a conserved peptide motif that is necessary for the autoproteolytic cleavage of vertebrate Nup98 (Parry et al., 2006): Because this sequence might contribute to the lack of fluorescence activity of DRA2-GFP, we generated a new version of the protein with GFP tags in both the C-terminal and N-terminal ends (35S:GFP-DRA2-GFP). Transient overexpression of this fusion in agroinfiltrated leaves of *N. benthamiana* showed green fluorescence in cytoplasm and nucleoplasm spots (Figure 6B, upper panels and S8B). The analysis of confocal series of optical sections further showed that unlike NtDRA2-GFP, GFP-DRA2-GFP fluorescence was detected in both the nuclear rim and inside the nucleus but excluded from the nucleolus (Figures 6B, lower panels and S8C). The observed

subcellular localization is consistent with DRA2 being part of the NPC and also fit with the idea that DRA2, like mNup98, is a dynamic NUP rather than just a key structural element of the NPC.

In summary, based on (i) the functionality and subcellular localization of the dominant negative NtDRA2-GFP protein, and (ii) the subcellular localization of full-length GFP-DRA2-GFP, we concluded that, like its mammalian counterpart mNup98, DRA2 is a dynamic NUP.

Beyond the nucleocytoplasmic transport: a dual role for the dynamic DRA2 in the SAS regulation?

Our work highlights the importance of the nucleocytoplasmic transport for the adaptation of plants to changing light environments (Figure 7). After phytochrome inactivation induced by perception of low R:FR light, increased dephosphorylation of PIF proteins, that likely causes enhanced DNA-binding to their target genes (Li et al., 2012), results in a rapid induction of expression of *PAR* genes, some of which encode transcriptional regulators that are instrumental for SAS responses. These changes, directly or indirectly, affect the endogenous hormonal pathways by altering the levels of or sensitivity to hormones, such as auxins, brassinosteroids and gibberellins (Li et al., 2012; Bou-Torrent et al., 2014). The NPC components SAR1 and SAR3 have been shown to play a role in auxin signaling and development (Parry et al., 2006). Although it is currently unknown whether DRA2 and other NUPs also play a role in auxin signaling, it is possible that the attenuated hypocotyl elongation in response to simulated shade shared by different NUP-defective mutants (Figures 1, 2, S5) might be related with general alterations in hormonal-regulated development caused by a transport-

dependent activity of the NPC (Figure 7). Further studies need to be done to explore this possibility.

Besides a role as part of the NPC, DRA2 has an additional and unique function as regulator of genes actively transcribed immediately after the shade stimulus perception. How can DRA2 affect shade-induced gene expression? We envisage two alternative mechanisms. Firstly, the dynamic nature of DRA2 might provide the protein with the ability to specifically alter nucleo-cytoplasmic movement of light-signaling components, such as phytochromes, known to partition between the cytoplasm and nucleus in a light-dependent manner. A defect in phytochrome partitioning would be expected to result in a global impairment of shade-regulated activities, such as the early induction of gene expression. However, shade-induced *HFR1*, *PHYB* and *PIL1* expression was impaired in *dra2-1* seedlings (Figure 4) but *ATHB2* expression was unaffected (Figure S7) despite the shade-induced expression of *ATHB2*, *PIL1* and other *PAR* genes has been shown to be affected by altered levels of phyA or phyB (Devlin et al., 2003; Roig-Villanova et al., 2006). We therefore believe that this first scenario is unlikely. A second possibility would be the control of gene expression by direct binding to the chromatin, as proposed for metazoan Nup98 (Light et al., 2013). This would represent a transport-independent mechanism in which DRA2 accesses chromatin regions corresponding to shade-induced genes (Figure 7). Work is in progress to explore this second possibility as a way to establish the precise molecular mechanisms by which DRA2 selectively influences transcription of early shade-regulated genes.

MATERIAL AND METHODS

Plant material and growth conditions

Arabidopsis plants for seed production and for the crosses were grown in the greenhouse as described (Martinez-Garcia et al., 2002). All the experiments were performed with seeds surface-sterilized and sown on Petri dishes with solid growth medium without sucrose [GM–; 0.215 % (w/v) MS salts plus vitamins, 0.025 % (w/v) MES pH 5.8] (Roig-Villanova et al., 2006), unless otherwise stated. After stratification (3–5 days) plates were incubated in a I-36VL growth chamber (Percival Scientific Inc, Perry, IA, USA) at 22ºC under W, that was provided by four cool-white vertical fluorescent tubes (25 $\mu mol \cdot m^{-2} \cdot s^{-1}$ of photosynthetically active radiation; R:FR ratio of 3.2-4.5). Simulated shade (W+FR) was generated by enriching W with supplementary FR provided by QB1310CS-670-735 light-emitting diode (LED) hybrid lamps (Quantum Devices Inc., Barneveld, WI, USA; http://www.quantumdev.com) (25 $\mu mol \cdot m^{-2} \cdot s^{-1}$ of photosynthetically active radiation; R:FR ratio of 0.05). Fluence rates were measured using an EPP2000 spectrometer (StellarNet Inc., USA, http://www.stellarnetinc.com/) or a Spectrosense2 meter associated with a 4-channel sensor (Skye Instruments Ltd., www.skyeinstruments.com) (Martinez-Garcia et al., 2014). For gene expression analyses seeds were sown on filter paper or a nylon mesh on top of GM–. For luciferase imaging, GM- media was supplemented with sucrose 2% (w/v).Supplemental Information provides a list of the mutants used in this work, accession numbers of the mutated genes, the molecular nature of their mutations, their genetic backgrounds and the sequences of the oligonucleotides used for their genotyping by PCR.

Seedling morphometry.

Hypocotyl, cotyledon and primary leaf lengths were measured as described (Roig-Villanova et al., 2007; Sorin et al., 2009). At least 15 seedlings were used for each treatment. Experiments were repeated 3–5 times and a representative one is shown. Statistical analyses of the data (one-way ANOVA with Tukey HSD post hoc comparison; and two-way ANOVA) were performed using GraphPad Prism version 4.00 for Windows (http://www.graphpad.com/).

Construction of transgenic lines

Transgenic 35S:DRA2-GFP and 35S:RNAi-DRA2 lines were in the Ws-2. Transgenic 35S:NtDRA2-GFP lines were in the Col-0 background. Details of their generation are given as supplementary information.

Gene expression analysis

Total RNA was isolated from seedlings using the RNAeasy® Plant Mini kit (Qiagen, http://www.qiagen.com) or the Maxwell® 16 LEV simplyRNA Tissue kit (Promega, www.promega.com). Reverse transcriptase and quantitative PCR (qPCR) analyses of gene expression were performed as indicated elsewhere (Sorin et al., 2009). The *UBQ10* gene was used as a control for normalizations. Three biological replicas for each sample were assayed. Primer sequences can be found in the Supplementary Data. Statistical analyses of the data (one-way ANOVA with Tukey HSD post hoc comparison; and two-way ANOVA) were performed using GraphPad Prism version 4.00 for Windows (http://www.graphpad.com/).

Whole-mount *in situ* hybridization of polyA RNA

Poly(A) RNA *in situ* hybridization was conducted essentially as described (Gong et al., 2005) with minor modifications, described as supplemental information.

Subcellular localization analyses

Confocal microscopy we performed in transgenic seedlings, bombarded leek epidermal cells or agroinfiltrated *Nicotiana benthamiana* leaves using either a Leica confocal microscope TCS SP5 II (Leica, www.leica.com) or an Olympus Confocal Microscope FV1000.2.4 (Olympus, www.olympus-lifescience.com). For GFP activity of transgenic seedlings (35S:DRA2-GFP and 35S:NtDRA2-GFP lines) at least two independent transgenic lines were examined for each construct. Details of the constructs and protocols used for the bombardments or the agroinfiltration are provided as supplemental information.

ACKNOWLEDGEMENTS

We are grateful to the greenhouse service for plant care; to Chus Burillo for technical help; to Sergi Portolés and Carles Rentero for helping in the mutagenesis; to Mark Estelle (UCSD, USA) for providing *sar1-4*, *sar3-1* and *sar3-3* seeds; to Juanjo López-Moya (CRAG, Barcelona; 35S:HcPro plasmid) and Dolors Ludevid (CRAG; C307 plasmid) for providing DNA plasmids; and to Manuel Rodríguez-Concepción (CRAG) and Miguel Blázquez (IBMCP) for comments on the manuscript. MG received a FPI fellowship from the Spanish Ministerio de Economía y Competitividad (MINECO); AG and AF-A received FPU fellowships from the Spanish Ministerio de Educación. SP received a FI fellowship from the Agència de Gestió D'ajuts Universitaris i de Recerca

(AGAUR - Generalitat de Catalunya). CT received a Marie Curie postdoctoral contract funded by the European Commission. IR-V received initially a FPI fellowship from the Spanish MINECO and later a Beatriu de Pinós contract from AGAUR. Our research is supported by grants from the Spanish MINECO-FEDER (BIO2008-00169, BIO2011-23489, BIO2014-59895-P) and Generalitat de Catalunya (2011-SGR447 and Xarba) to JFM-G, and Generalitat Valenciana (PROMETEO/2009/112, PROMETEOII/2014/006) to MRP and JLM.

AUTHOR CONTRIBUTIONS

MG, AG, SP, CT, AF-A, LL-O, IR-V, XW, JLM, MRP, PFD and JFM-G performed experiments and data analyses; MG, AG, SP, CT, MRP and JFM-G prepared the manuscript and LL-O, IR-V, JLM and PFD contributed with their comments to the final version of the manuscript.

REFERENCES

Bae, G. and Choi, G. (2008). Decoding of light signals by plant phytochromes and their interacting proteins, *Annu Rev Plant Biol* **59**: 281-311.

Bou-Torrent, J., Galstyan, A., Gallemi, M., Cifuentes-Esquivel, N., Molina-Contreras, M. J., Salla-Martret, M., Jikumaru, Y., Yamaguchi, S., Kamiya, Y. and Martinez-Garcia, J. F. (2014). Plant proximity perception dynamically modulates hormone levels and sensitivity in Arabidopsis, *J Exp Bot* **65**(11): 2937-2947.

Bou-Torrent, J., Roig-Villanova, I., Galstyan, A. and Martinez-Garcia, J. F. (2008). PAR1 and PAR2 integrate shade and hormone transcriptional networks, *Plant Signal Behav* **3**(7): 453-4.

Bou-Torrent, J., Toledo-Ortiz, G., Ortiz-Alcaide, M., Cifuentes-Esquivel, N., Halliday, K. J., Martinez-Garcia, J. F. and Rodriguez-Concepcion, M. (2015). Regulation of carotenoid biosynthesis by shade relies on specific subsets of antagonistic transcription factors and co-factors, *Plant Physiol* **169**(3): 1584-94.

Capelson, M. and Hetzer, M. W. (2009). The role of nuclear pores in gene regulation, development and disease, *The EMBO Reports* **10**(7): 697-705.

Capelson, M., Liang, Y., Schulte, R., Mair, W., Wagner, U. and Hetzer, M. W. (2010). Chromatin-bound nuclear pore components regulate gene expression in higher eukaryotes, *Cell* **140**(3): 372-83.

Cifuentes-Esquivel, N., Bou-Torrent, J., Galstyan, A., Gallemi, M., Sessa, G., Salla Martret, M., Roig-Villanova, I., Ruberti, I. and Martinez-Garcia, J. F. (2013). The bHLH proteins BEE and BIM positively modulate the shade avoidance syndrome in Arabidopsis seedlings, *The Plant Journal* **75**(6): 989-1002.

Crocco, C. D., Holm, M., Yanovsky, M. J. and Botto, J. F. (2010). AtBBX21 and COP1 genetically interact in the regulation of shade avoidance, *The Plant Journal* **64**(4): 551-562.

D'Angelo, M. A., Raices, M., Panowski, S. H. and Hetzer, M. W. (2009). Age-dependent deterioration of nuclear pore complexes causes a loss of nuclear integrity in postmitotic cells, *Cell* **136**(2): 284-95.

Devlin, P. F., Yanovsky, M. J. and Kay, S. A. (2003). A genomic analysis of the shade avoidance response in Arabidopsis, *Plant Physiol* **133**(4): 1617-29.

Dong, C. H., Hu, X., Tang, W., Zheng, X., Kim, Y. S., Lee, B. H. and Zhu, J. K. (2006). A putative Arabidopsis nucleoporin, AtNUP160, is critical for RNA export and required for plant tolerance to cold stress, *Mol Cell Biol* **26**(24): 9533-43.

Ferrandez-Ayela, A., Alonso-Peral, M. M., Sanchez-Garcia, A. B., Micol-Ponce, R., Perez-Perez, J. M., Micol, J. L. and Ponce, M. R. (2013). Arabidopsis TRANSCURVATA1 Encodes NUP58, a Component of the Nucleopore Central Channel, *PLoS One* **8**(6): e67661.

Fontoura, B. M., Blobel, G. and Yaseen, N. R. (2000). The nucleoporin Nup98 is a site for GDP/GTP exchange on ran and termination of karyopherin beta 2-mediated nuclear import, *J Biol Chem* **275**(40): 31289-96.

Franklin, K. A. (2008). Shade avoidance, *New Phytol* **179**(4): 930-944.

Gangappa, S. N., Crocco, C. D., Johansson, H., Datta, S., Hettiarachchi, C., Holm, M. and Botto, J. F. (2013). The Arabidopsis B-BOX Protein BBX25 Interacts with HY5, Negatively Regulating BBX22 Expression to Suppress Seedling Photomorphogenesis, *The Plant Cell* **25**(4): 1243-1257.

Gong, Z., Dong, C. H., Lee, H., Zhu, J., Xiong, L., Gong, D., Stevenson, B. and Zhu, J. K. (2005). A DEAD box RNA helicase is essential for mRNA export and

important for development and stress responses in Arabidopsis, *The Plant Cell* **17**(1): 256-67.

Griffis, E. R., Altan, N., Lippincott-Schwartz, J. and Powers, M. A. (2002). Nup98 is a mobile nucleoporin with transcription-dependent dynamics, *Mol Biol Cell* **13**(4): 1282-97.

Hodel, A. E., Hodel, M. R., Griffis, E. R., Hennig, K. A., Ratner, G. A., Xu, S. and Powers, M. A. (2002). The three-dimensional structure of the autoproteolytic, nuclear pore-targeting domain of the human nucleoporin Nup98, *Mol Cell* **10**(2): 347-58.

Jacob, Y., Mongkolsiriwatana, C., Veley, K. M., Kim, S. Y. and Michaels, S. D. (2007). The nuclear pore protein AtTPR is required for RNA homeostasis, flowering time, and auxin signaling, *Plant Physiol* **144**(3): 1383-90.

Josse, E. M., Foreman, J. and Halliday, K. J. (2008). Paths through the phytochrome network, *Plant, Cell and Environment* **31**(5): 667-78.

Kalverda, B., Pickersgill, H., Shloma, V. V. and Fornerod, M. (2010). Nucleoporins directly stimulate expression of developmental and cell-cycle genes inside the nucleoplasm, *Cell* **140**(3): 360-71.

Keuskamp, D. H., Sasidharan, R. and Pierik, R. (2010). Physiological regulation and functional significance of shade avoidance responses to neighbors, *Plant Signal Behav* **5**(6): 655-662.

Kozma-Bognar, L., Hall, A., Adam, E., Thain, S. C., Nagy, F. and Millar, A. J. (1999). The circadian clock controls the expression pattern of the circadian input photoreceptor, phytochrome B, *Proceedings of the National Academy of Sciences, USA* **96**(25): 14652-7.

Leivar, P. and Quail, P. H. (2011). PIFs: pivotal components in a cellular signaling hub, *Trends Plant Sci* **16**(1): 19-28.

Li, L., Ljung, K., Breton, G., Schmitz, R. J., Pruneda-Paz, J., Cowing-Zitron, C., Cole, B. J., Ivans, L. J., Pedmale, U. V., Jung, H. S. et al. (2012). Linking photoreceptor excitation to changes in plant architecture, *Genes and Development* **26**(8): 785-790.

Liang, Y., Franks, T. M., Marchetto, M. C., Gage, F. H. and Hetzer, M. W. (2013). Dynamic association of NUP98 with the human genome, *PLoS Genet* **9**(2): e1003308.

Light, W. H., Freaney, J., Sood, V., Thompson, A., D'Urso, A., Horvath, C. M. and Brickner, J. H. (2013). A conserved role for human Nup98 in altering chromatin structure and promoting epigenetic transcriptional memory, *PLoS Biol* **11**(3): e1001524.

Lorrain, S., Allen, T., Duek, P. D., Whitelam, G. C. and Fankhauser, C. (2008). Phytochrome-mediated inhibition of shade avoidance involves degradation of growth-promoting bHLH transcription factors, *The Plant Journal* **53**(2): 312-23.

MacGregor, D. R., Gould, P., Foreman, J., Griffiths, J., Bird, S., Page, R., Stewart, K., Steel, G., Young, J., Paszkiewicz, K. et al. (2013). HIGH EXPRESSION OF OSMOTICALLY RESPONSIVE GENES1 is required for circadian periodicity through the promotion of nucleo-cytoplasmic mRNA export in Arabidopsis, *Plant Cell* **25**(11): 4391-404.

Martinez-Garcia, J. F., Galstyan, A., Salla-Martret, M., Cifuentes-Esquivel, N., Gallemí, M. and Bou-Torrent, J. (2010). Regulatory components of shade avoidance syndrome, *Advances in Botanical Research* **53**: 65-116.

Martinez-Garcia, J. F., Gallemi, M., Molina-Contreras, M. J., Llorente, B., Bevilaqua, M. R. and Quail, P. H. (2014). The shade avoidance syndrome in Arabidopsis: the antagonistic role of phytochrome a and B differentiates vegetation proximity and canopy shade, *PLoS One* **9**(10): e109275.

Martinez-Garcia, J. F., Huq, E. and Quail, P. H. (2000). Direct targeting of light signals to a promoter element-bound transcription factor, *Science* **288**(5467): 859-63.

Martinez-Garcia, J. F., Virgos-Soler, A. and Prat, S. (2002). Control of photoperiod-regulated tuberization in potato by the Arabidopsis flowering-time gene CONSTANS, *Proceedings of the National Academy of Sciences, USA* **99**(23): 15211-6.

Parry, G. (2013). Assessing the function of the plant nuclear pore complex and the search for specificity, *J Exp Bot* **64**(4): 833-45.

Parry, G. (2014). Components of the Arabidopsis nuclear pore complex play multiple diverse roles in control of plant growth, *J Exp Bot* **65**(20): 6057-67.

Parry, G., Ward, S., Cernac, A., Dharmasiri, S. and Estelle, M. (2006). The Arabidopsis SUPPRESSOR OF AUXIN RESISTANCE proteins are nucleoporins with an important role in hormone signaling and development, *The Plant Cell* **18**(7): 1590-603.

Powers, M. A., Forbes, D. J., Dahlberg, J. E. and Lund, E. (1997). The vertebrate GLFG nucleoporin, Nup98, is an essential component of multiple RNA export pathways, *J Cell Biol* **136**(2): 241-50.

Radu, A., Moore, M. S. and Blobel, G. (1995). The peptide repeat domain of nucleoporin Nup98 functions as a docking site in transport across the nuclear pore complex, *Cell* **81**(2): 215-22.

Raices, M. and D'Angelo, M. A. (2012). Nuclear pore complex composition: a new regulator of tissue-specific and developmental functions, *Nat Rev Mol Cell Biol* **13**(11): 687-99.

Roig-Villanova, I., Bou-Torrent, J., Galstyan, A., Carretero-Paulet, L., Portoles, S., Rodriguez-Concepcion, M. and Martinez-Garcia, J. F. (2007). Interaction of shade

avoidance and auxin responses: a role for two novel atypical bHLH proteins, *Embo J* **26**(22): 4756-67.

Roig-Villanova, I., Bou, J., Sorin, C., Devlin, P. F. and Martinez-Garcia, J. F. (2006). Identification of primary target genes of phytochrome signaling. Early transcriptional control during shade avoidance responses in Arabidopsis, *Plant Physiology* **141**(1): 85-96.

Salter, M. G., Franklin, K. A. and Whitelam, G. C. (2003). Gating of the rapid shade-avoidance response by the circadian clock in plants, *Nature* **426**(6967): 680-3.

Sessa, G., Carabelli, M., Sassi, M., Ciolfi, A., Possenti, M., Mittempergher, F., Becker, J., Morelli, G. and Ruberti, I. (2005). A dynamic balance between gene activation and repression regulates the shade avoidance response in Arabidopsis, *Genes and Development* **19**(23): 2811-5.

Singer, S., Zhao, R., Barsotti, A. M., Ouwehand, A., Fazollahi, M., Coutavas, E., Breuhahn, K., Neumann, O., Longerich, T., Pusterla, T. et al. (2012). Nuclear pore component Nup98 is a potential tumor suppressor and regulates posttranscriptional expression of select p53 target genes, *Mol Cell* **48**(5): 799-810.

Smith, H. (1982). Light quality, photoperception, and plant strategy, *Annu Rev Plant Physiol* **33**: 481-518.

Smith, H. and Whitelam, G. (1997). The shade avoidance syndrome: multiple responses mediated by multiple phytochromes, *Plant, Cell and Environment* **20**(6): 840-844.

Sorin, C., Salla-Martret, M., Bou-Torrent, J., Roig-Villanova, I. and Martinez-Garcia, J. F. (2009). ATHB4, a regulator of shade avoidance, modulates hormone response in Arabidopsis seedlings, *The Plant Journal* **59**(2): 266-77.

Tamura, K., Fukao, Y., Iwamoto, M., Haraguchi, T. and Hara-Nishimura, I. (2011). Identification and Characterization of Nuclear Pore Complex Components in Arabidopsis thaliana, *The Plant Cell*.

Tamura, K. and Hara-Nishimura, I. (2013). The molecular architecture of the plant nuclear pore complex, *J Exp Bot* **64**(4): 823-32.

Wang, X., Roig-Villanova, I., Khan, S., Shanahan, H., Quail, P. H., Martinez-Garcia, J. F. and Devlin, P. F. (2011). A novel high-throughput in vivo molecular screen for shade avoidance mutants identifies a novel phyA mutation, *J Exp Bot* **62**(8): 2973-87.

Xu, X. M. and Meier, I. (2008). The nuclear pore comes to the fore, *Trends in Plant Sciences* **13**(1): 20-7.

Xu, X. M., Meulia, T. and Meier, I. (2007). Anchorage of plant RanGAP to the nuclear envelope involves novel nuclear-pore-associated proteins, *Current Biology* **17**(13): 1157-63.

Zhao, Q. and Meier, I. (2011). Identification and characterization of the Arabidopsis FG-repeat nucleoporin Nup62, *Plant Signal Behav* **6**(3): 330-4.

Figures

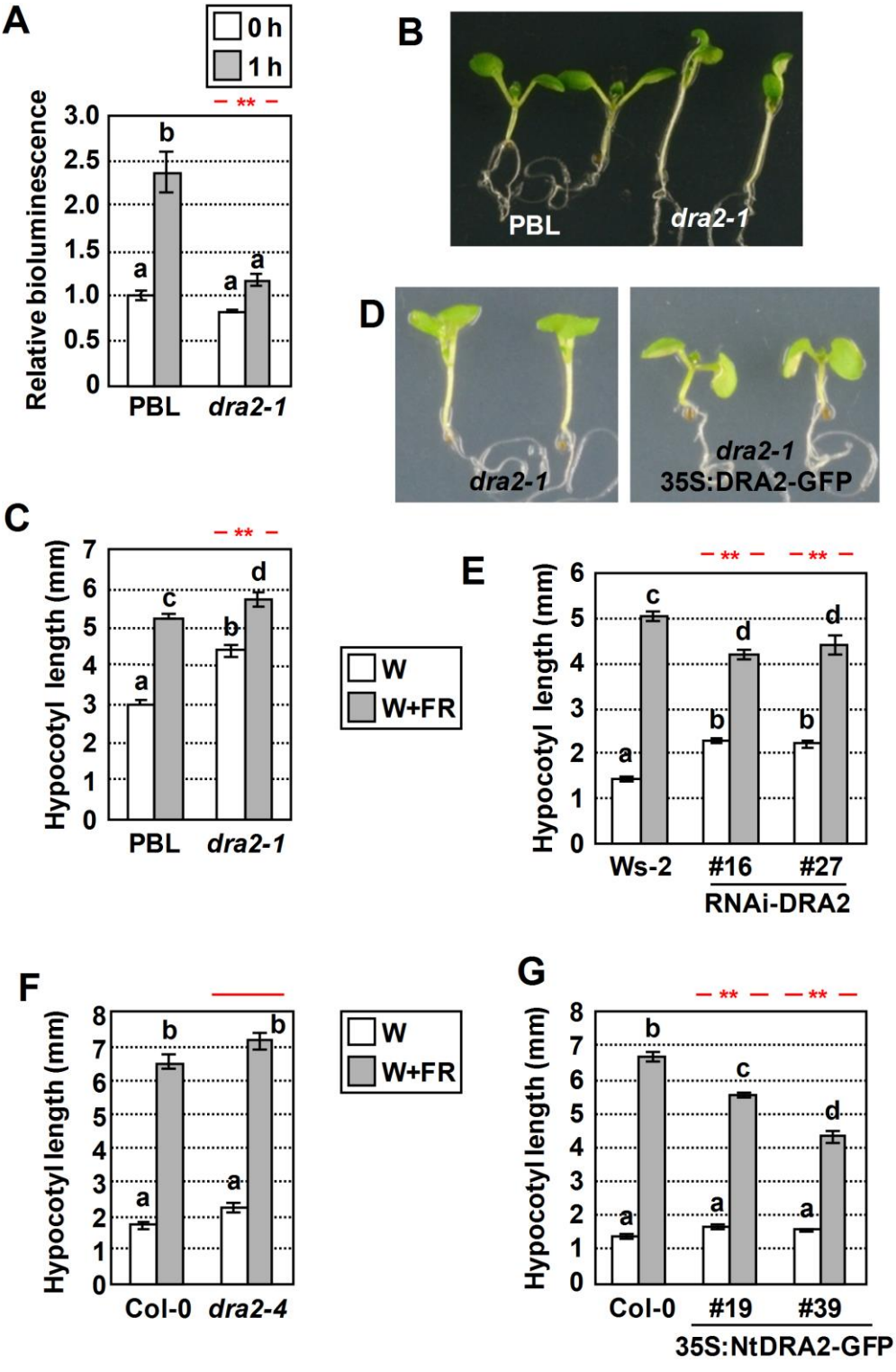

Figure 1. *dra2-1* seedlings show a reduced response to simulated shade. **(A)** Seven-day-old white light (W)-grown seedlings of PBL and *dra2-1* (0 h) were transferred to W+FR for 1 h. Data represent mean bioluminescence measurements ± SE from at least 20 seedlings relative to the activity levels in PBL seedlings at 0 h. **(B)** Representative 7-day-old PBL and *dra2-1* seedlings grown under W. **(C)** Length of hypocotyls of PBL and *dra2-1* in response to W+FR. Seeds were germinated and grown for 2 days under W and then either kept under W or transferred to W+FR for 5 more days. **(D)** Representative 7-day-old seedlings of *dra2-1* (left) and *dra2-1*;35S:DRA2-GFP (right). **(E)** Hypocotyl length of wild-type (Ws-2) and transgenic 35S:RNAi-DRA2 seedlings in response to simulated shade. **(F)** Hypocotyl length of wild-type (Col-0) and mutant *dra2-4* seedlings; and **(G)** transgenic 35S:NtDRA2-GFP seedlings in response to simulated shade. In sections **A**, **C**, **E**, **F** and **G**, different letters denote significant differences (one-way ANOVA with Tukey test, $P<0.05$) among means; and red asterisks indicate significant differences (two-way ANOVA, *$P<0.05$, **$P<0.01$) between the mutant and wild-type genotypes in response to W+FR.

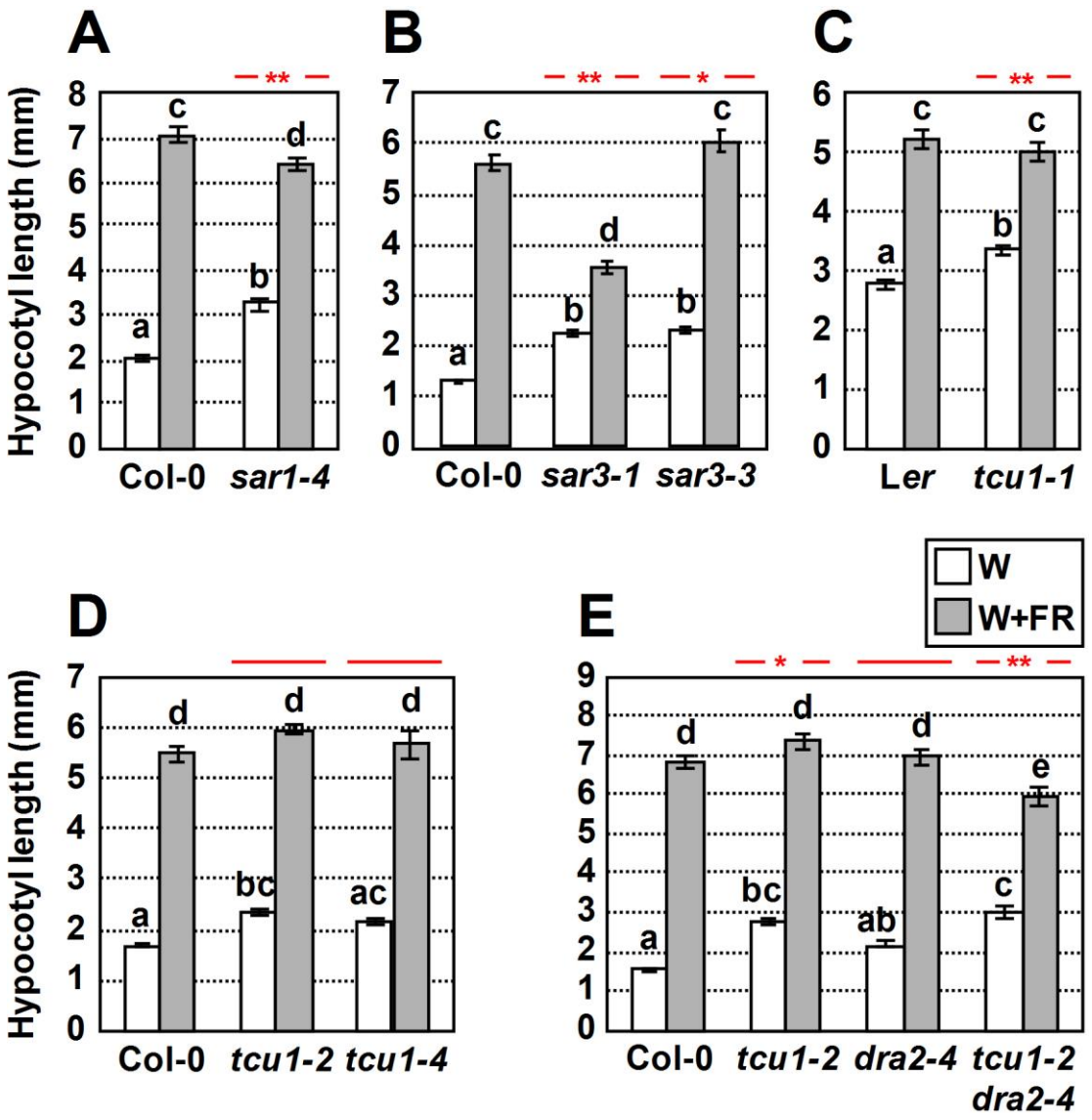

Figure 2. Seedlings deficient in several NUPs show an altered response to simulated shade. Hypocotyl (Hyp) length of wild-type (Col-0 and Ler) and **(A)** mutant *sar1-4*, **(B)** *sar3-1, sar3-3*, **(C)** *tcu1-1*, **(D)** *tcu1-2* and *tcu1-4* seedlings in response to simulated shade. **(E)** Genetic analysis of functional redundancy between *TCU1* and *DRA2* in Col-0 ecotype. Hyp length of wild-type, *tcu1-2*, *dra2-4* and *tcu1-2;dra2-4* mutants in response to simulated shade. Seedlings were grown as indicated in Figure 1C. Different letters denote significant differences (one-way ANOVA with Tukey test, $P<0.05$)

among means. Red asterisks indicate significant differences (two-way ANOVA, *P<0.05, **P<0.01) between the mutant and wild-type genotypes in response to W+FR.

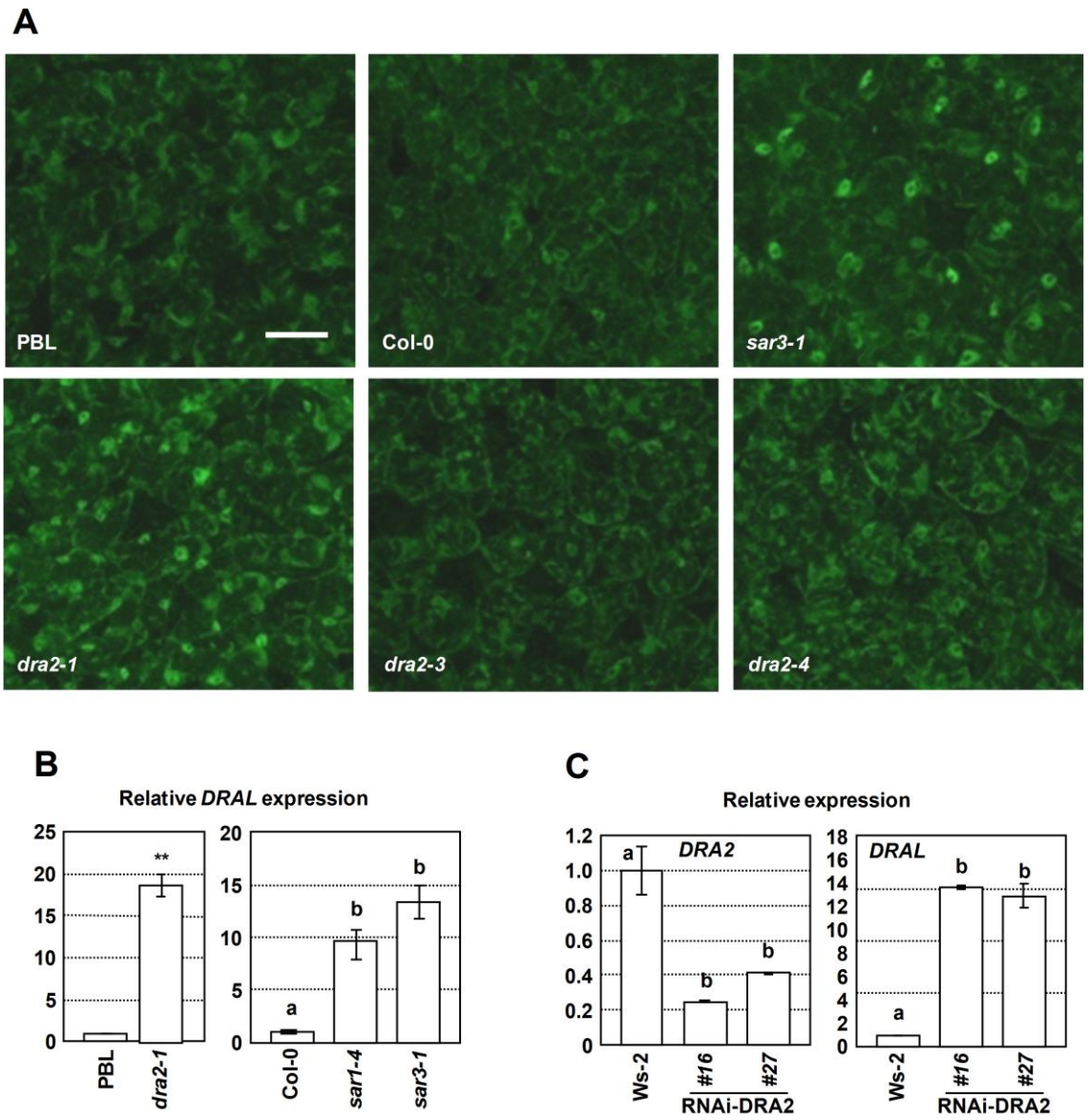

Figure 3. Several NUP-deficient mutants display similar defects in export of mRNA and changes in *DRAL* gene expression. **(A)** *In situ* hybridization of polyA$^+$-RNA was performed in cotyledons of 7-day-old seedlings grown under white light. Seedlings from wild-type (Col-0, Ws-2), *dra2-1*, *sar3-1*, *dra2-3* and *dra2-4* mutants were analyzed with oligo(dT)-fluorescein-tagged probe. Fluorescence was visualized by confocal microscopy. Bar = 40µm. **(B)** *DRAL* gene expression analysis in seedlings of wild-type (PBL or Col-0), *dra2-1*, *sar1-4* and *sar3-1* mutants. Seedlings were grown under continuous W for 7 days. **(C)** *DRA2* and *DRAL* gene expression analysis in

seedlings of wild-type (Ws-2) and the two RNAi-DRA2 independent transgenic lines shown in Figure 1E. In sections **B** and **C**, seedlings were grown under continuous W for 7 days. Transcript abundance of *DRAL* and *DRA2* (both normalized to *UBQ10*) is shown. Values are means ± SE of 3-6 independent biological replicates relative to wild-type values. In sections **B** and **C**, asterisks indicate significant differences (Student's *t*-test, **P<0.01) relative to the wild-type seedlings, and different letters denote significant differences (one-way ANOVA with Tukey test, P<0.05) among means.

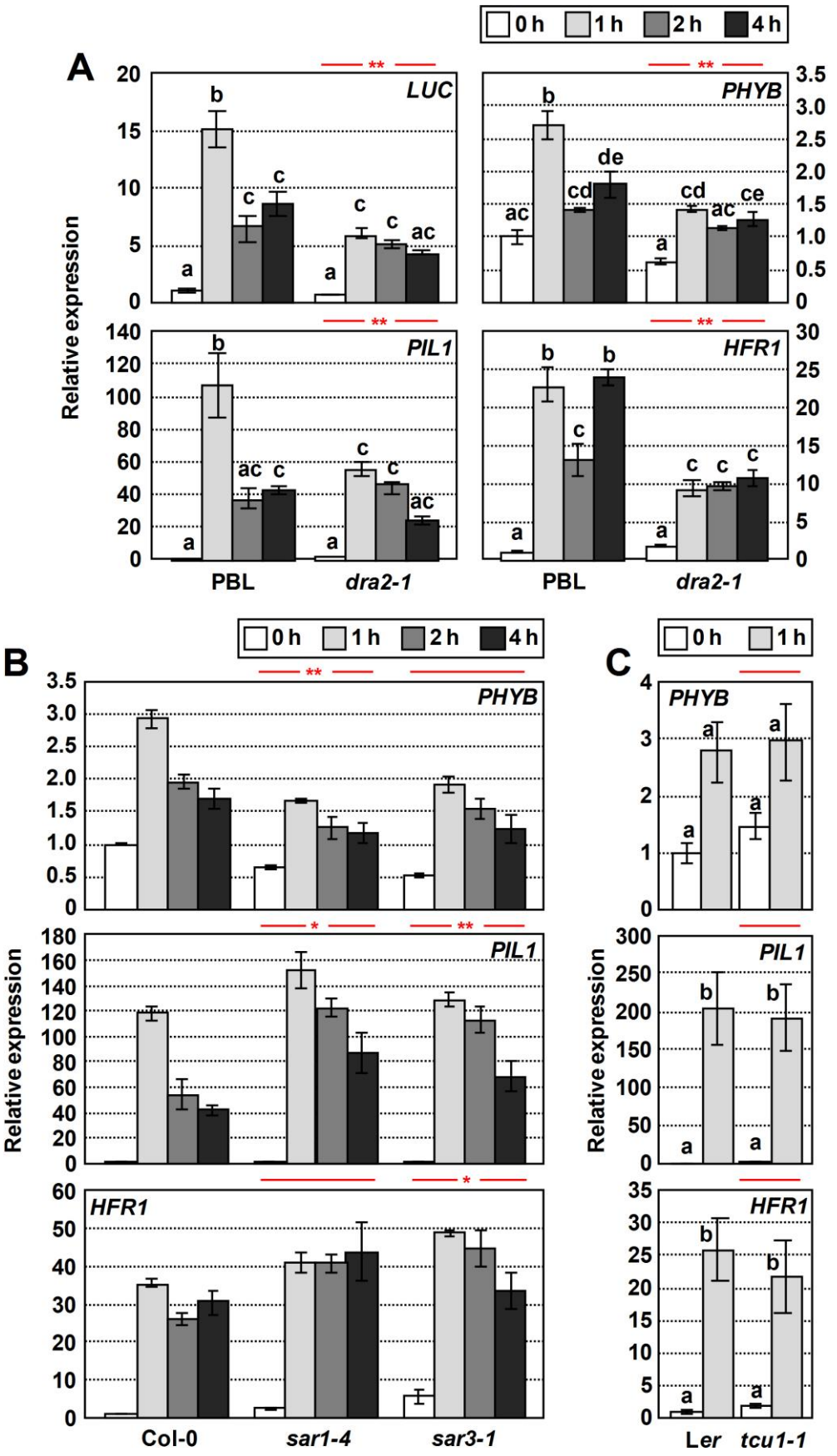

Figure 4. Shade-induced expression is attenuated on *dra2-1* but not on other NUP mutants. **(A)** Expression analysis of *PAR* genes in seedlings of wild-type (PBL or Col-0) **(A)**, *dra2-1*, **(B)** *sar1-4* or *sar3-1* seedlings treated for 0, 1, 2 and 4 h with W+FR. **(C)** Expression analysis of *PAR* genes in wild-type (L*er*) and *tcu1-1* seedlings treated for 0 and 1 h with W+FR. Seedlings were grown under continuous W for 7 days. Transcript abundances, normalized to *UBQ10*, for the indicated genes, are shown. Values are means ± SE of three independent quantitative PCR biological replicates relative to wild-type values at 0 h. In sections **A** and **C**, different letters denote significant differences (one-way ANOVA with Tukey test, $P<0.05$) among means. In section **B**, the results of the one-way ANOVA with Tukey test ($P<0.05$) are presented in Table S2. Red asterisks indicate significant differences (two-way ANOVA, *$P<0.05$, **$P<0.01$) between the mutant and wild-type genotypes in response to W+FR.

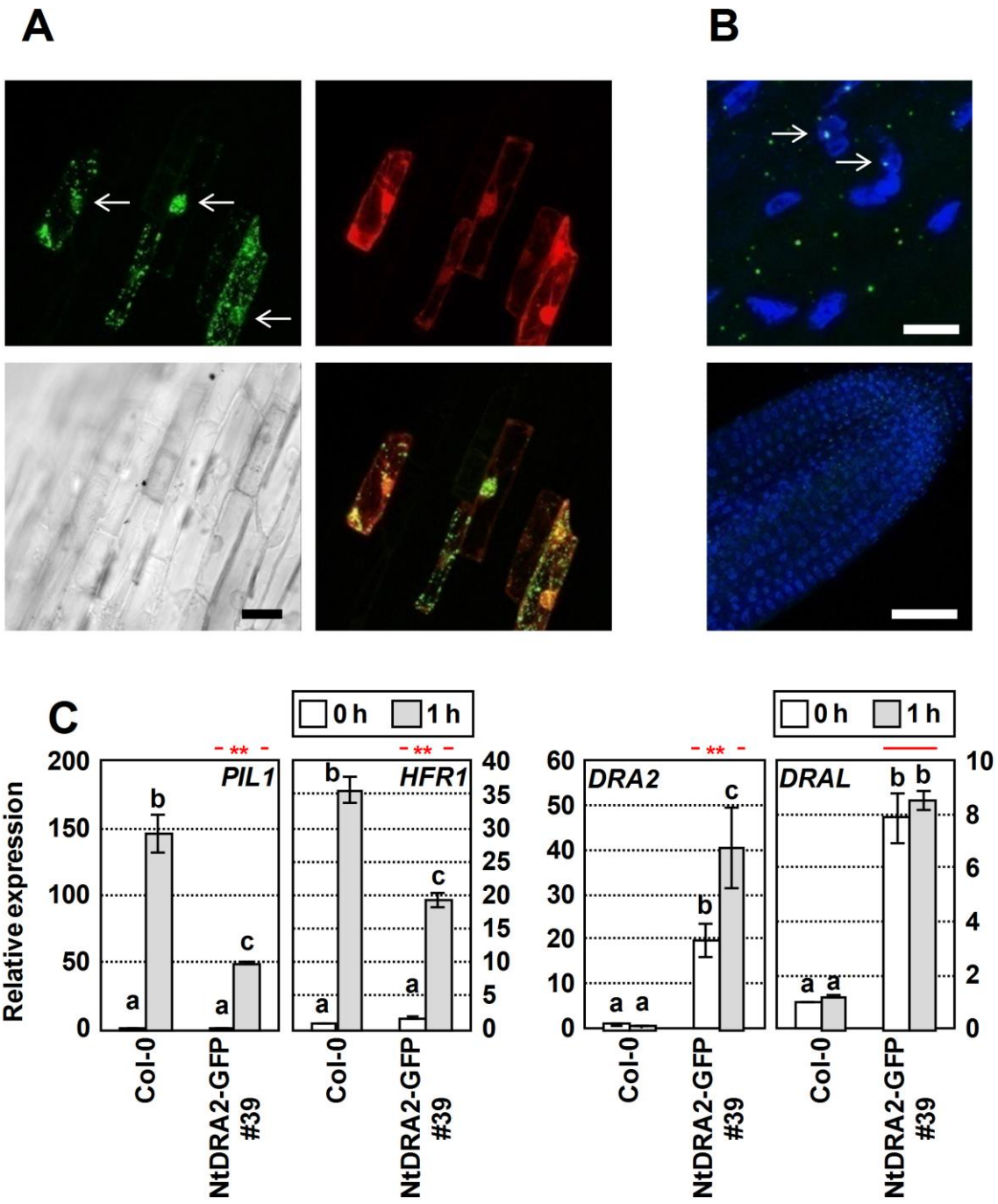

Figure 5. NtDRA2 acts as a dominant negative form. Subcellular location of the NtDRA2-GFP fusion protein in **(A)** leek onion epidermal cells (scale bar = 50 µm) and **(B)** roots of transgenic Arabidopsis seedlings (upper scale bar = 50 µm, lower scale bar = 10 µm). In section **A**, leek cells were co-bombarded with constructs encoding NtDRA2-GFP and DsRED, a red fluorescent protein. Fluorescence was analyzed after

24 h. Green (upper left), red (upper right), overlay fluorescence (lower right) and bright-field images (lower left) are shown. In section **B**, roots correspond to 35S:NtDRA2-GFP seedlings grown under continuous W for 7 days; root cells were stained using DAPI to identify nuclei (shown in light blue color). In sections **A** and **B**, arrows point to the GFP activity located in nuclei. **(C)** Expression analysis of *PIL1*, *HFR1*, *DRA2* and *DRAL* in wild-type and 35S:NtDRA2-GFP seedlings treated for 0 and 1 h with W+FR. Seedlings were grown under continuous W for 7 days. Transcript abundances were analyzed as indicated in Figure 4. In section **C**, different letters denote significant differences (one-way ANOVA with Tukey test, $P<0.05$) among means; red asterisks indicate significant differences (two-way ANOVA, *$P<0.05$, **$P<0.01$) between the transgenic and wild-type genotypes in response to W+FR.

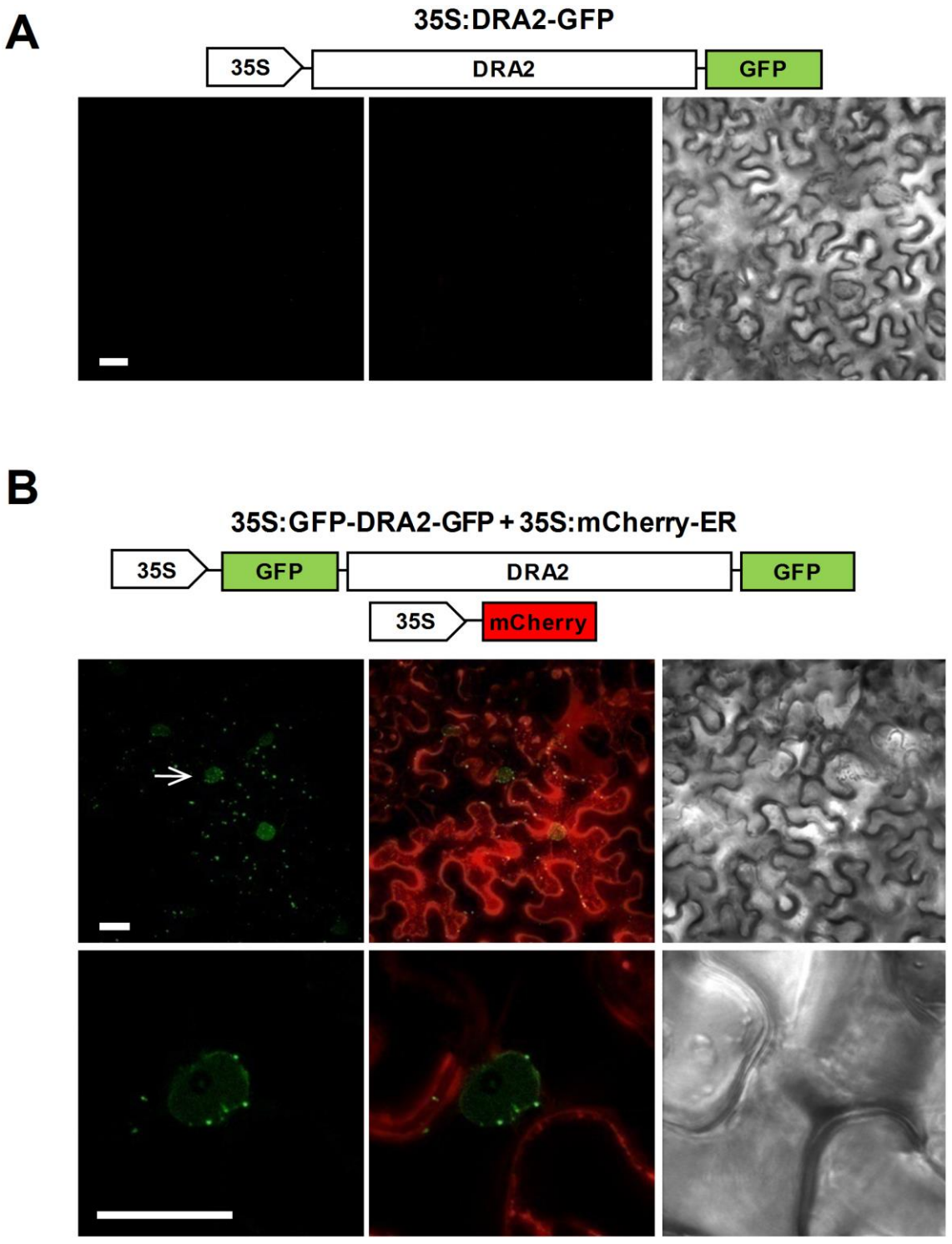

Figure 6. DRA2 is localized in the cytoplasm, the nucleoplasm and the nuclear rim. **(A)** Confocal images of leaf tobacco cells agroinfiltrated with construct DRA2-GFP. Cartoon of the construct used is shown at the top of the section. **(B)** Confocal images of leaf tobacco cells co-agroinfiltrated with constructs GFP-DRA2-GFP and mCherry-ER.

Cartoon detailing the constructs used is shown at the top of the panel. The 3 upper images are the Z stack of 10 optical sections. Arrow points to the nucleus magnified in the 3 lower images, which correspond to a single and intermediate optical section (see Figure S8). In each series of three images, green fluorescence (left), red and green fluorescence overlay (centre), and bright-field images (right) are shown. In each series, images are shown to the same scale. Scale bars = 20 μm.

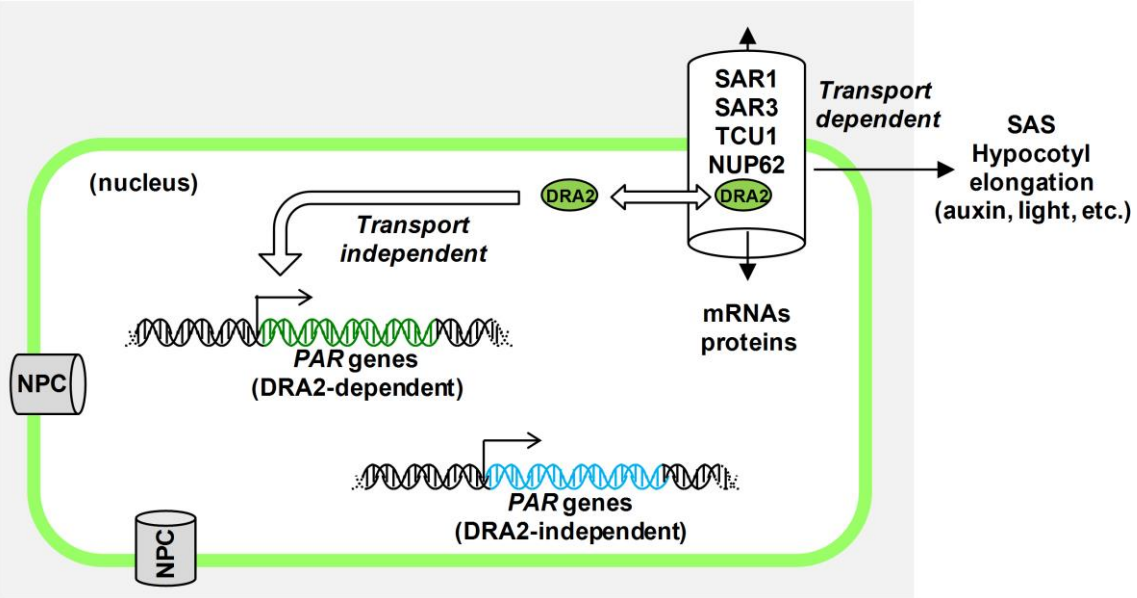

Figure 7. Model representing the dual role of DRA2 in regulating different aspects of the SAS in seedlings: a transport-dependent function on the regulation of SAS hypocotyl elongation, shared with several other NPC components (such as SAR1, SAR3, TCU1 and NUP62, analyzed in this work), and a transport-independent function on the regulation of shade-induced gene expression, postulated as unique of DRA2. The latter function is likely related to the dynamism of DRA2, which can shuttle between the NPC, located in the nuclear envelope, and the nucleus and cytoplams.